Eur Biophys J (2007) 36:173–185
DOI 10.1007/s00249-006-0115-1

ORIGINAL PAPER

Electropermeabilization of dense cell suspensions

Gorazd Pucihar · Tadej Kotnik · Justin Teissié · Damijan Miklavčič

Received: 24 August 2006 / Revised: 8 November 2006 / Accepted: 17 November 2006 / Published online: 9 February 2007

Abstract This paper investigates the influence of cell density on cell membrane electropermeabilization. The experiments were performed on dense cell suspensions (up to 400×10^6 cells/ml), which represent a simple model for studying electropermeabilization of tissues. Permeabilization was assayed with a fluorescence test using Propidium iodide to obtain the mean number of permeabilized cells (i.e. fluorescence positive) and the mean fluorescence per cell (amount of loaded dye). In our study, as the cell density increased from 10×10^6 to 400×10^6 cells/ml, the fraction of permeabilized cells decreased by approximately 50%. We attributed this to the changes in the local electric field, which led to a decrease in the amplitude of the induced transmembrane voltage. To obtain the same fraction of cell permeabilization in suspensions with 10×10^6 and 400×10^6 cells/ml, the latter suspension had to be permeabilized with higher pulse amplitude, which is in qualitative agreement with numerical computations. The electroloading of the cells also decreased with cell density. The decrease was considerably larger than expected from the differences in the permeabilized cell fractions alone. The additional decrease in fluorescence was mainly due to cell swelling after permeabilization, which reduced extracellular dye availability to the permeabilized membrane and hindered the dye diffusion into the cells. We also observed that resealing of cells appeared to be slower in dense suspensions, which can be attributed to cell swelling resulting from electropermeabilization.

Keywords Electroporation · Cell pellets · Propidium iodide · Membrane resealing

List of symbols

$\Delta\Psi$	induced transmembrane voltage, V
R	cell radius, m
E	applied electric field, V/m
φ	angle between E and the normal vector to the membrane, °
φ_c	critical angle where permeabilization occurs, °
E_S	critical amplitude of the electric field, V/m
A_{perm}	permeabilized surface of the membrane, m^2
A_{tot}	total area of the membrane, m^2
α	angle, °
Φ	flow of molecules, mol/s
P	permeability coefficient, m/s
ΔS	concentration difference of the molecule S, mol/m^3
$F(\mathrm{t})$	fraction of membrane defects in the permeabilized region, –
$F^*(N,T)$	fraction of membrane defects immediately after the onset of permeabilizing pulse, –
t	time, s
N	number of pulses, –
T	pulse duration, s
k	resealing rate, 1/s
F_{NC}	fraction of permeabilized surface where cell contacts are not present, –

G. Pucihar · T. Kotnik · D. Miklavčič
Faculty of Electrical Engineering, University of Ljubljana, Tržaška 25, 1000 Ljubljana, Slovenia

J. Teissié (✉)
IPBS, CNRS, UMR 5089, 205 Route de Narbonne, Toulouse Cedex, France
e-mail: justin.teissie@ipbs.fr

c	total concentration of PI after permeabilization (cells + external medium), mol/m^3
c_1	concentration of PI in external medium, mol/m^3
V	total volume (cells + external medium), m^3
V_1	volume of external medium, m^3
EMEM	eagle's minimum essential medium, –
PI	propidium iodide, –
CHO	Chinese hamster ovary cells, –

Introduction

Exposure of cells to an electric field of sufficient amplitude leads to an increased permeability of cell membranes, a phenomenon termed electropermeabilization (electroporation) (Tsong 1991; Barnett and Weaver 1991; Weaver and Chizmadzhev 1996; Teissié et al. 1999; Neumann et al. 1999). Electropermeabilization occurs in the regions of the membrane where the transmembrane voltage, induced by the external electric field, exceeds a certain threshold characteristic for each cell line. Provided that the amplitude of the field is not too high and the duration not too long, the increase in permeability is reversible, and cells return to their initial state after the exposure.

During the state of high permeability it is possible to deliver membrane-impermeant ions and molecules (e.g. various drugs, DNA) into cells. With a reversible permeabilization and sufficiently rapid resealing of the membrane, this method is very efficient, and during the last two decades it has found an increasing use in drug delivery to tumor cells—electrochemotherapy (Okino and Mohri 1987; Serša et al. 1995; Mir and Orlowski 1999; Gothelf et al. 2003; Šatkauskas et al. 2005) and gene delivery to cells—electrogenetherapy (Neumann et al. 1982; Šatkauskas et al. 2002; Čemažar et al. 2003; Fattori et al. 2005).

Despite the increasing use of electropermeabilization, the events on the molecular scale that result in the increase in membrane permeability are not completely understood even in such simplified membrane models as pure lipid bilayers. For biological cells, the mechanisms of electropermeabilization are better understood in diluted cell suspensions than in tissues, where irregular shapes of the cells, their mutual electric shielding, and perhaps connections between them (e.g. gap junctions) play a role. As a consequence, it is more difficult to plan, without prior experiments, an efficient and safe electropermeabilization protocol for cells in tissues than for suspensions. For one reason, the induced transmembrane voltage for cells in suspension can be calculated analytically, while for cells in tissues, which are irregularly shaped, numerical computing is required (see e.g. Pucihar et al. 2006). To gain understanding of tissue electropermeabilization, the researchers often use—both in theoretical analysis and in experiments—simple models of tissues, such as dense cell suspensions, cell pellets or multicellular spheroids (Abidor et al. 1993, 1994; Susil et al. 1998; Schmeer et al. 2004; Pavlin et al. 2002; Canatella et al. 2004). Here and throughout this paper, ''cell density'' should be understood as the volume fraction that the cells occupy in the suspension and a ''dense suspension'' is a suspension in which the cell density is considerable. These studies suggest that if cells are relatively close to each other, they respond to the electric field differently from isolated cells. Condensation of cells changes their response to electropulsation. Indeed, in two recent theoretical studies the authors showed that the amplitude of transmembrane voltage induced on spherical cells progressively decreases when cells are brought closer together (Susil et al. 1998; Pavlin et al. 2002). Because permeabilization is observed in the regions of the membrane where the induced transmembrane voltage exceeds a threshold value, the increased cell density should, according to these theoretical studies, lead to a decrease in cell permeabilization. In addition, an experimental study on multicellular spheroids showed that the uptake of molecules to cells after permeabilization is lower and spatially more heterogeneous in such spheroids than in isolated cells (Canatella et al. 2004). The observed differences in uptake were attributed to cell size distribution (cells in the interior of the spheroids were smaller than cells on the periphery), slow diffusion of the dye to the cells inside the spheroids, limited extracellular solute reservoir, and heterogeneous field strength due to influence of neighbouring cells.

The purpose of the study presented in this paper was to investigate the effect of the mutual electrical shielding of cells on the process of cell electropermeabilization. The experiments were performed on cell suspensions, because they presented an easy and controlled system, which could also be treated theoretically. Besides, the cell size distribution was uniform over the whole suspension and the dye distribution in suspension was homogeneous. This enabled the observation of the changes in cell permeabilization, resulting only from the electrical shielding of cells. Together with numerical computations of the induced transmembrane voltage, the results of our study provide a complement to the theoretical and experimental studies presented before.

Materials and methods

Cells

The experiments were performed on Chinese hamster ovary cells (CHO cells, WTT clone), which were grown in EMEM medium (MEM 0111, Eurobio, France) with added fetal calf serum (8%, Boehringer, Germany), antibiotics (penicillin 100 units/ml, streptomycin 100 μg/ml) and L-glutamine (1.16 mg/ml). The cells were kept in suspension by gentle, continuous agitation (100 rpm) in spinner flasks at 37°C. The key advantage of the WTT clone of CHO cells is that the cells are growing in suspension, so no trypsin treatment is needed and the extracellular matrix remains intact. Light scattering studies by flow cytometry did not show considerable cell clustering resulting from spinning of suspension. Prior to the experiments, part of the suspension was taken from the spinner to determine the cell density (usually 1.5×10^6 cells/ml), and then the suspension (4×50 ml) was centrifuged (200×*g*, 5 min, Jouan C 500 centrifuge, France). After centrifugation, the supernatant was replaced with pulsing buffer (10 mM KH_2PO_4/K_2HPO_4, 250 mM sucrose, 1 mM $MgCl_2$), which contained 100 μM of fluorescent dye propidium iodide (PI, Sigma, St Louis, USA), to obtain cell density of 400×10^6 cells/ml. When the buffer was added, the volume of the pellet was taken into account and was thus subtracted from the calculated volume. The suspension was gently pipetted a few times with a large tip pipet to obtain a homogenous dye distribution. We should note that 400×10^6 cells/ml results in a very dense but still liquid suspension. A part of the suspension with 400×10^6 cells/ml was then further diluted with the same dye-containing buffer to obtain cell densities of 200×10^6 and 10×10^6 cells/ml. The volume fractions of cells in these cell densities were approximately 36, 18, and 1%, respectively [the average radii of CHO cell is about 6 μm (Golzio et al. 1998)]. Cells were kept at 4°C before exposure to electric pulses. Only limited cell damages were associated to these manipulations.

Electropermeabilization

Cell suspension (100 μl) was placed between two parallel, flat, stainless steel electrodes placed 5 mm apart. The electrodes were connected to a Jouan electropulsator (Jouan, St Herblain, France) and to an oscilloscope (Enertec, St Etienne, France), where pulse delivery was continuously monitored. Two different pulse protocols were used: 8×100 μs rectangular pulses (short pulses), a typical electropermeabilization protocol, and a 10×5 ms rectangular pulses (long pulses), a protocol, which induces membrane perturbations supporting gene transfer. In both protocols, the pulses were delivered with 1 Hz repetition frequency. After electropermeabilization cells were incubated for 7 min at 25°C and then resuspended in 1 ml of D-PBS (Gibco, USA).

Detection of electropermeabilization

Cells were pulsed in the presence of PI, a non-permeant fluorescent dye, which emits strong fluorescence after entering the permeabilized or damaged cells. The percentage of permeabilized cells and the mean fluorescence intensity of the cells were determined from the histograms obtained by flow cytometry (FACscan, Becton-Dickinson, USA) as shown in Fig. 1a, b. On the histogram of the pulsed sample (cells exposed to electric pulses), the position of two markers (M1 and M2) was selected at the apparent boundary between the population of nonpermeabilized (M1) and permeabilized cells (M2) as shown in Fig. 1b. The fraction of permeabilized cells was then given by the percentage of cells in the M2 window, while the fluorescence of the cells was represented by the mean fluorescence of the whole sample (M1 and M2). The position of the markers was kept the same for all investigated parameters within one experiment. Intact cells of the control sample (85% of the population) were in the M1 section (Fig. 1a).

Resealing of cells after electropermeabilization

The cells were prepared as described above, except that propidium iodide was mixed into cell suspension

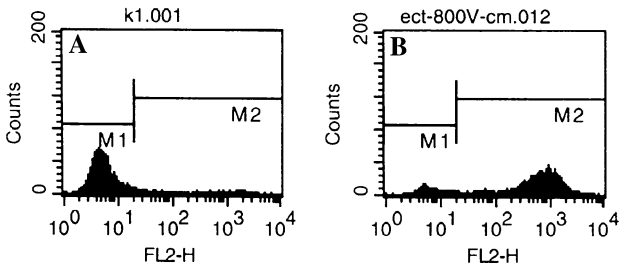

Fig. 1 The histogram of the fluorescence of the cells. M1 and M2 mark the nonpermeabilized and permeabilized cells, respectively, for **a** the control sample, and **b** electropermeabilization with 800 V/cm, 8×100 μs pulses. The fraction of permeabilized cells was given by the percentage of cells within the range of M2. The fluorescence of the cells was represented by the mean fluorescence of the whole sample (M1 and M2)

at specific times after the pulse delivery. The experiments were first performed in 10×10^6 cells/ml suspension, where the dye was added 0, 10, 30 s, 1, 3, 5, and 7 min after permeabilization. Specifically, at a given time, 100 µl of dye in pulsing buffer was added to 100 µl of cell suspension to obtain 100 µM final concentration of the dye in cell suspension. From the results, the times at which roughly 0, 50, and 100% of the cells resealed were determined and at these specific times, the resealing of cells in 400×10^6 cells/ml suspension was then measured. The dye was added in the same manner as described for dilute suspensions. In experiments where the dense suspension was diluted after permeabilization with 900 µl of the pulsing buffer, 100 µl of 1.1 mM PI was added at specific times after permeabilization to obtain 100 µM final concentration of the dye in suspension. In all cases, the suspensions were carefully pipetted a few times with a large tip pipet to obtain homogenous distribution of the dye in suspension. In dense suspension, the resealing was measured only at three specific times because a large number of cells would be required to perform the same experiment with dilute and dense cell suspension. The resealing is known to obey first-order kinetics (Rols and Teissié 1990; Neumann et al. 1998).

After permeabilization, the cells were incubated for 7 min at 25°C, except for the cells to which the dye was added 7 min after pulsation, which were incubated for two additional minutes. The subsequent cell handling and the detection of permeabilization were the same as described above.

Theoretical background

Isolated cells, cells in dilute suspensions

When a cell is exposed to an external electric field E, a transmembrane voltage $\Delta\Psi$ is induced across its membrane. For an isolated spherical cell in physiological conditions, this voltage can be calculated from the following equation (Schwan 1957; Pauly and Schwan 1959; Grosse and Schwan 1992; Kotnik et al. 1997):

$$\Delta\Psi = 1.5 \cdot R \cdot E \cdot \cos\varphi, \tag{1}$$

where R is the cell radius and φ is the angle between the electric field and the normal vector to the membrane. At certain amplitude of the external electric field (E_S), the transmembrane voltage reaches critical amplitude and electropermeabilization is detected. Because $\Delta\Psi$ varies with the position on the cell membrane, the permeabilization first occurs in the regions of the membrane facing the electrodes ($|\cos\ \varphi| = 1$). For $E > E_S$, the relation between E and E_S can be written as (Rols and Teissié 1990):

$$E_s = E \cdot \cos\varphi_c, \tag{2}$$

where φ_c is the angle characterizing the permeabilized cap of the membrane (A_{perm}). This region can be calculated by integrating the equation:

$$\mathrm{d}A_{\text{perm}} = R \cdot \mathrm{d}\alpha \cdot 2\pi \cdot R \cdot \sin\ \alpha, \tag{3}$$

where α varies from 0 to φ_c, and introducing the total area of the membrane (A_{tot}):

$$A_{\text{perm}} = 1/2 \cdot A_{\text{tot}} \cdot (1 - E_S/E); \quad \text{for } E > E_S. \tag{4}$$

Membrane-impermeable ions and molecules can enter the cell through the permeabilized region of the membrane (A_{perm}) with the flow (Φ), which can be described by using the modified First law of Fick:

$$\Phi = P \cdot F \cdot A_{\text{perm}} \cdot \Delta S. \tag{5}$$

In this equation, P denotes the permeability coefficient in the defects of the membrane for molecule S, F is a fraction of defects in the permeabilized region and ΔS is the concentration difference of the molecule between cell interior and exterior. Taking into account the above equations and under the assumption that the extracellular volume is an infinite reservoir compared to the cytoplasmic volumes, the flux of the molecule S at time t after the pulse can therefore be expressed as:

$$\Phi(S,t) = 1/2 \cdot P \cdot \Delta S(t) \cdot F(t) \cdot A_{\text{tot}} \cdot (1 - E_S/E), \tag{6}$$

where $\Delta S(t)$ is the concentration difference of the molecule S at time t. The fraction of defects in the permeabilized region, $F(t)$, can be written as:

$$F(t) = F^*(T, N) \cdot \mathrm{e}^{-k \cdot t} \tag{7}$$

where F^*, the density of defects instantaneously resulting from the pulses, is a function of only the pulse duration (T) and the number of pulses (N), (resealing is not present if the frequency of pulses is high enough as in our experimental conditions), k, the resealing rate, is a function of pulse duration (T), number of pulses (N) (Rols and Teissié 1990, 1998) and osmotic conditions (Golzio et al. 1998) and t is the time elapsed after electropermeabilization. Electroloading is obtained by the integral of $\Phi(S, t)$ during the permeabilized lifetime. Under these conditions, at given E, T, N, cell size and $\Delta S(0)$, electroloading is controlled by k.

Cells in dense suspensions

When a cell is in a dense suspension it is close to its neighbouring cells, which alter the local electric field around it. As a consequence, the amplitude of $\Delta\Psi$ decreases and its spatial distribution changes, so that it becomes flatter in the regions of the cell facing the electrodes (Susil et al. 1998; Pavlin et al. 2002). The analytical solution for $\Delta\Psi$ obtained for an isolated cell (Eq. 1) is therefore not valid anymore and $\Delta\Psi$ in dense suspensions can be calculated only numerically (Susil et al. 1998; Pavlin et al. 2002). Also, the extracellular volume cannot be considered as an infinite reservoir compared to the cytoplasmic volumes anymore. The change in $\Delta S(t)$ after permeabilization may be affected.

Numerical calculations of $\Delta\Psi$ on cells in dense suspensions

The influence of volume fraction of cells and their arrangements in suspension on $\Delta\Psi$ was studied in a paper published by Pavlin et al. (2002). Here, we computed $\Delta\Psi$ for the specific experimental conditions and volume fractions of cells used in our study (1, 18, and 36%). Although the arrangement of cells in suspension is random, on a large scale it can be approximated by a face-centered cubic lattice, where cells are located in the corners and in faces of a cube (Fig. 2a). Detailed information on the methodology of the computation of the induced transmembrane voltage on cubic lattices can be found in (Susil et al. 1998; Pavlin et al. 2002). Numerical computations were performed with finite elements modeling software Femlab 3.1 (COMSOL Inc., Burlington, MA, USA) using DC application mode. As the results in Fig. 2b show, the maximum amplitude of $\Delta\Psi$ normalized to the radius R and electric field E decreases from the value of 1.5 for an isolated cell to 1.493, 1.39, and 1.32, for 1% (solid line), 18% (dotted line), and 36% (dashed line) volume fractions of cells in suspension, respectively.

The flow of molecules (Φ) through the permeabilized cell membrane can be derived from Eq. 5. The permeabilized surface (A_{perm}) in this case can be calculated numerically, by integration over the part of the cell surface where $\Delta\Psi$ is above the critical value. Because cells are in close contact, (due to the high density of suspension or due to cell swelling after permeabilization), the flow mostly occurs on the fraction of the permeabilized surface where such contacts are not present (F_{NC}):

$$\Phi(S,t) = P \cdot \Delta S \cdot F_{NC} \cdot F \cdot A_{\text{perm}}. \quad (8)$$

Compared to isolated cells or dilute cell suspensions, the flow of molecules and the resulting electroloading are decreased, because A_{perm} is smaller (due to lower $\Delta\Psi$) and also because $F_{\text{NC}} < 1$.

Results

Determination of pulse amplitudes for electropermeabilization

To investigate the efficiency of electropermeabilization as a function of cell density we first determined the pulse amplitude that led to a detectable electropermeabilization of cells in these suspensions. For this

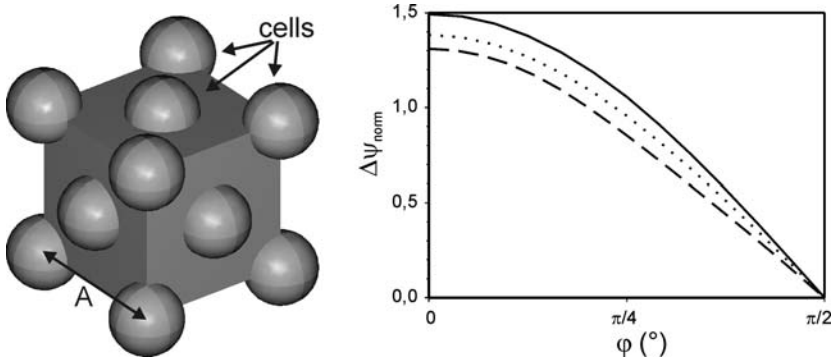

Fig. 2 **a** Model of cell suspension with cells arranged in a face-centered cubic lattice. A is the length of the side of the cube. The cube represents the extracellular medium with specific conductivity 0.14 S/m (Rols et al. 1998), while the cells were modeled as nonconductive solid spheres. The remaining sides of the cube were insulating, to model the infinite lattice of cells. **b** $\Delta\Psi$ on cells arranged in the lattice for volume fractions of 1% *solid line*, 18% *dotted line*, and 36% *dashed line*. $\Delta\Psi$ was normalized to the cell radius and the electric field. Due to symmetry, only one quarter of the distribution of $\Delta\Psi$ is shown. The values of $\Delta\Psi$ were calculated in steps smaller than 0.5°, points were connected with a smooth curve

purpose we performed the measurements of cell permeabilization as a function of the pulse amplitude (expressed by the ratio of the voltage applied to the electrodes and the distance between them). Since an increase in cell density can generally be expected to reduce the level of electropermeabilization (see Introduction), we performed these initial experiments on a suspension with the lowest cell density (10×10^6 cells/ml). The results of electropermeabilization as a function of the pulse amplitude for 8×100 μs (short pulses) and 10×5 ms (long pulses) are shown in Fig. 3a. Two typical electropermeabilization curves were obtained, showing almost no change from the control up to certain amplitudes, then a relatively sharp increase in the fraction of permeabilized cells, and finally a plateau where practically all cells were permeabilized. Compared to the electropermeabilization curve for short pulses, the curve for long pulses is shifted towards lower pulse amplitudes, reflecting the effect of longer pulse duration (Rols and Teissié 1998). From these two curves, the pulse amplitudes that caused the permeabilization of ~70% of the cells were estimated. For short and long pulses these voltage-to-distance amplitudes were approximately 700 and 400 V/cm, respectively.

Applying the same amplitudes on denser cell suspensions would allow detecting expected reduction in electropermeabilization resulting from an increase in cell density.

Fig. 3b shows the fluorescence of the cells as a function of the pulse amplitude. Similar to the permeabilization curves, we detected almost no increase in fluorescence at low pulse amplitudes, where cells are not yet permeabilized. As the amplitude increases, so does the fluorescence, until reaching a plateau that reflects the maximum level of permeabilization and the occupation of binding sites for the fluorescence dye. Similar limiting fluorescence was observed on the plateau conditions, whatever the pulse duration, suggesting the same loading of PI (Fig. 3b).

Electropermeabilization as a function of cell density

Initial experiments

Suspensions with three different cell densities, containing 10×10^6, 200×10^6, and 400×10^6 cells/ml, were exposed to electric pulses with the amplitudes yielding permeabilization of ~70% of the diluted cells for each of the two protocols (400 and 700 V/cm, see the preceeding section). The fraction of permeabilized cells as a function of cell density for the two protocols is shown in Fig. 4a, b. The relation between cell density and permeabilization was similar for both pulse protocols, namely an increase in cell density corresponding to a significant decrease in the fraction of permeabilized cells at the same pulse amplitude. More precisely, with an increase in cell density from 10×10^6 to 400×10^6 cells/ml, the fraction of permeabilized cells is reduced from 81 to 42% in the case of short 700 V/cm pulses, and from 65 to 24% in the case of long 400 V/cm pulses. The permeabilization in the control sample (10×10^6 cells/ml, 15%) reflects the cells that were damaged or lost their viability during the preparation.

Figure 4c, d show the fluorescence of permeabilized cells as a function of cell density. For both pulse protocols, the fluorescence was the strongest in the suspension containing 10×10^6 cells/ml, and the weakest in the suspension with 400×10^6 cells/ml.

In addition, experiments with short pulses were also performed with 1 mM concentration of PI, to verify if the extracellular reservoir of the dye affects the measurements. The results presented in Fig. 5 show the same tendency as those obtained with a 100 μM concentration. The fraction of cell permeabilization and the fluorescence both decrease with an increase in cell density, and the decrease is similar to the one observed with low PI concentration (100 μM, Fig. 5a, b). With 1 mM dye, the 40% of cells detected as permeabilized in the control group is due to the diffusion through

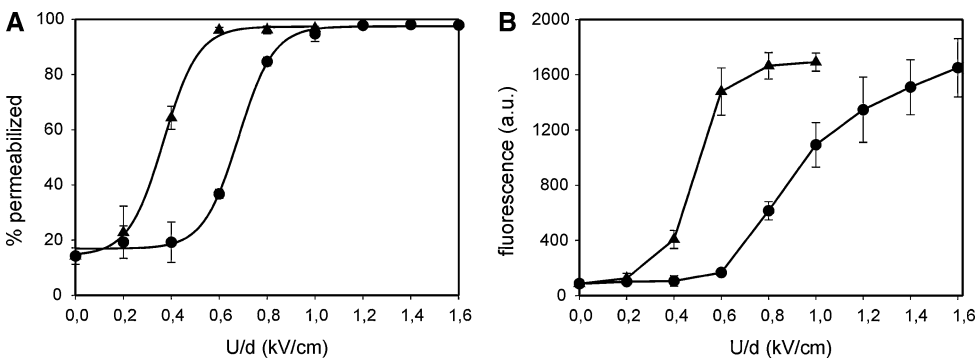

Fig. 3 **a** Electropermeabilization, and **b** fluorescence as a function of voltage-to-distance ratio for 8×100 μs (*black circles*) and 10×5 ms pulse protocol (*black triangles*). The density of cell suspension is 10×10^6 cells/ml. Each point in the figure represents the mean ± SD ($n = 3$)

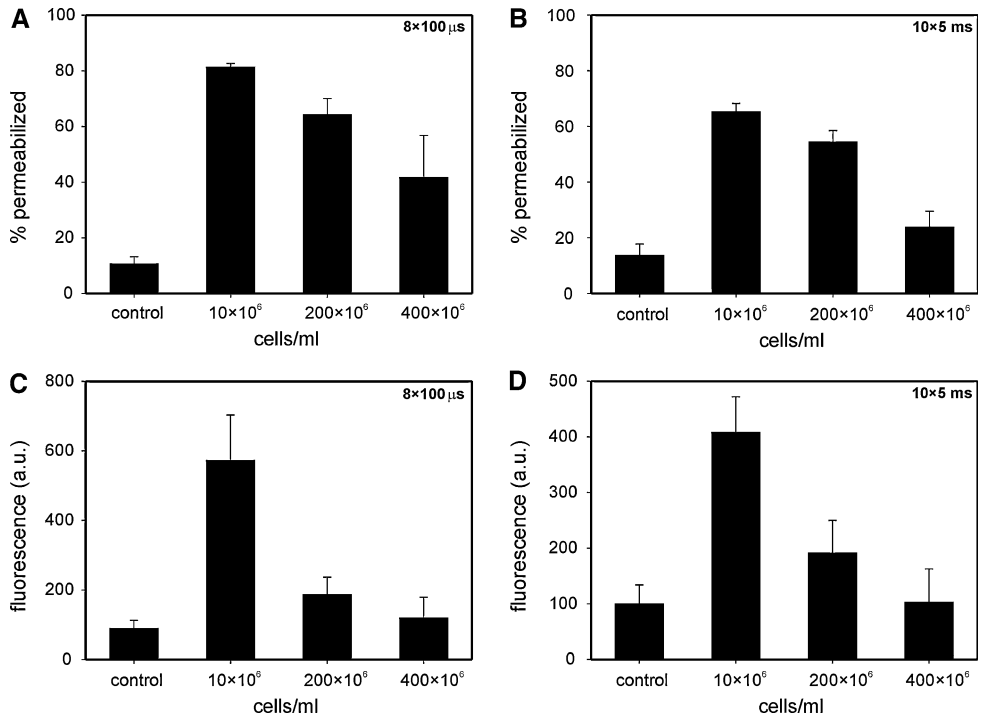

Fig. 4 Electropermeabilization as a function of cell density for **a** 8×100 μs (700 V/cm) and **b** 10×5 ms (400 V/cm) pulse protocol. Fluorescence as a function of cell density for **c** 8×100 μs (700 V/cm) and **d** 10×5 ms (400 V/cm) pulse protocol. Each column represents the mean ± SD ($n = 3$)

intact membranes, which becomes pronounced due to the very high dye concentration. Because of higher dye concentration and consequently higher fluorescence intensity, the parameters of the flow cytometer and the markers on the histogram (see Materials and methods) were adjusted.

A closer examination of the fluorescence in cell suspensions with different densities and comparison with permeabilization results show that the decrease in the fluorescence is more pronounced than would be expected from the differences in the fractions of permeabilized cells. This can be observed in the experiment with 100 μM and 1 mM dye concentration. Namely, as seen in Fig. 4a for example, the fractions of permeabilized cells in suspensions containing 200×10^6 and 400×10^6 cells/ml were approximately 80 and 50% of the fraction of permeabilized cells in the suspension with 10×10^6 cells/ml. Therefore, we would expect that the fluorescence in dense suspensions (200 and 400×10^6 cells/ml) would also decrease to roughly 80 and 50%, respectively, of the fluorescence in suspension with 10×10^6 cells/ml, but the observed fluorescence decrease was significantly larger (down to approximately 30 and 20%).

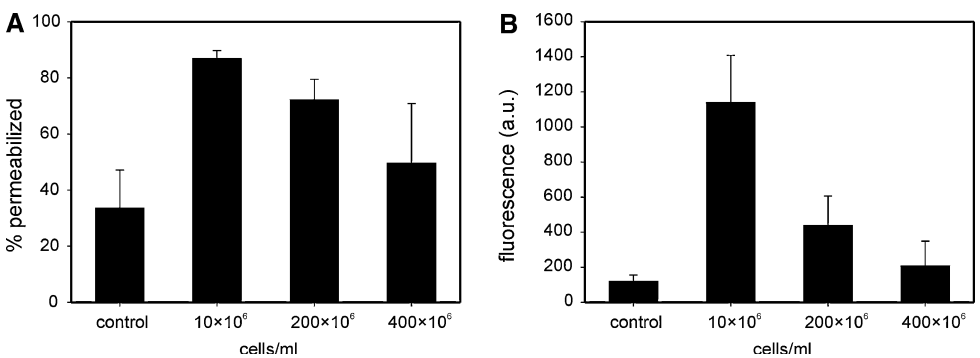

Fig. 5 **a** Electropermeabilization, and **b** fluorescence as a function of cell density for 8×100 μs (700 V/cm) pulse protocol and higher dye concentration (1 mM). Each column represents the mean ± SD ($n = 3$)

Two plausible explanations may be suggested for the observed fluorescence decrease. One is the dilution of the dye after permeabilization. Namely, in dense suspensions, cells represent a considerable part of the total volume of the suspension (e.g. 36% for 400×10^6 cells/ml), which means that the extracellular volume cannot be considered as an infinite reservoir of the dye anymore. Permeabilization allows the dye to enter the cells, which results in a decrease in the dye concentration outside the cell by an amount corresponding to the volume fraction represented by the cells. This dilution effect is negligible for the 10×10^6 cells/ml suspension, as the cells represent only 1% of the total volume of the suspension, but not for the 400×10^6 cells/ml suspension, where the volume fraction of cells is approximately 36%. The second possible explanation for the decrease in the fluorescence in dense suspensions could be cell swelling after electropermeabilization (Abidor et al. 1993, 1994; Canatella et al. 2004; Kinosita and Tsong 1977). After electropermeabilization in a sufficiently dense suspension, the volume represented by the cells could increase to a value where the cells come into close contact (similar to the situation in tissues), which would then limit the part of the permeabilized cell surface available for the transfer of PI, resulting in lower fluorescence (as explained in the theoretical background section).

We investigate these two plausible explanations in subsequent sections of this paper. Because the largest differences in the fraction of cell permeabilization and the fluorescence were observed between suspensions with 10×10^6 and 400×10^6 cells/ml, these investigations were performed only with these two suspensions. Also, to avoid the decrease in the fluorescence in dense suspension resulting from the decrease in the fraction of cell permeabilization in this suspension, we adjusted the pulse amplitudes to obtain roughly the same fraction of permeabilized cells in both cell density suspensions.

Compensation for dye dilution

Cells were permeabilized with pulse amplitudes yielding roughly the same fraction of permeabilization in the dilute and in the dense cell suspension. This was obtained from our experimental observations. In this manner, with short pulses the amplitude was 700 V/cm for 10×10^6 cells/ml, and 900 V/cm for 400×10^6 cells/ml. Similarly, with long pulses the amplitude was 400 V/cm for 10×10^6 cells/ml, and 540 V/cm for 400×10^6 cells/ml. Also, the concentration of the dye (c_1) in dense suspension was increased to 156 μM, to account for the decrease in external volume outside of the cells (from 99 down to 64%) ($c_1 \times V_1 = c \times V$; $c_1 = 100\ \mu M \times 1/0.64$). Namely, increasing the concentration of PI in dense suspension from 100 to 156 μM provided the final concentration of the dye after permeabilization (that is in extracellular and intracellular volume) equal to the concentration of the dye in dilute suspension (100 μM). The dilution of the dye in 10×10^6 cells/ml suspension was neglected due to the small volume fraction of cells in this suspension (1%).

As shown in Fig. 6, the modifications (increased pulse amplitude and compensation for the dye dilution) result in similar permeabilization of the population, but have a limited effect on the fluorescence in dense suspension. It remains considerably lower than the fluorescence in dilute suspension for both pulse protocols (e.g. compare the fluorescence of 400×10^6 cells/ml suspension in Fig. 6c, black column and grey columns).

Compensation for possible cell swelling

This experiment was similar to the one described in the previous subsection, except that immediately after electropermeabilization, the cell suspension (100 μl) was resuspended in 900 μl of pulsing medium with 100 μM dye concentration. If we assume that cells after permeabilization increase in their size, this results in a dramatic effect in case of dense suspensions, where the volume represented by the cells could increase to a value where the cells are in close contact. By dilution after the pulses we can avoid a long duration of these induced intercellular contacts.

The experiments were performed only for short pulses and the results (Fig. 7) are in agreement with our hypothesis. If the pulse amplitude was adjusted to achieve roughly the same fraction of cell permeabilization in suspensions with 10×10^6 and 400×10^6 cells/ml, the fluorescence of dense suspension diluted after permeabilization (denoted with letter D in superscript, grey hatched column in Fig. 7b), increased and approached the fluorescence of 10×10^6 cells/ml suspension (black hatched column in Fig. 7b). The fluorescence of dense cell suspension, which was not diluted after permeabilization, remained low (Fig. 7b, grey column). The fraction of cells detected as permeabilized in the dense suspension was slightly increased with dilution (Fig. 7a), which may result from a facilitated dye uptake. The remaining difference in fluorescence between the suspensions could be attributed to the slower resealing of cells after permeabilization.

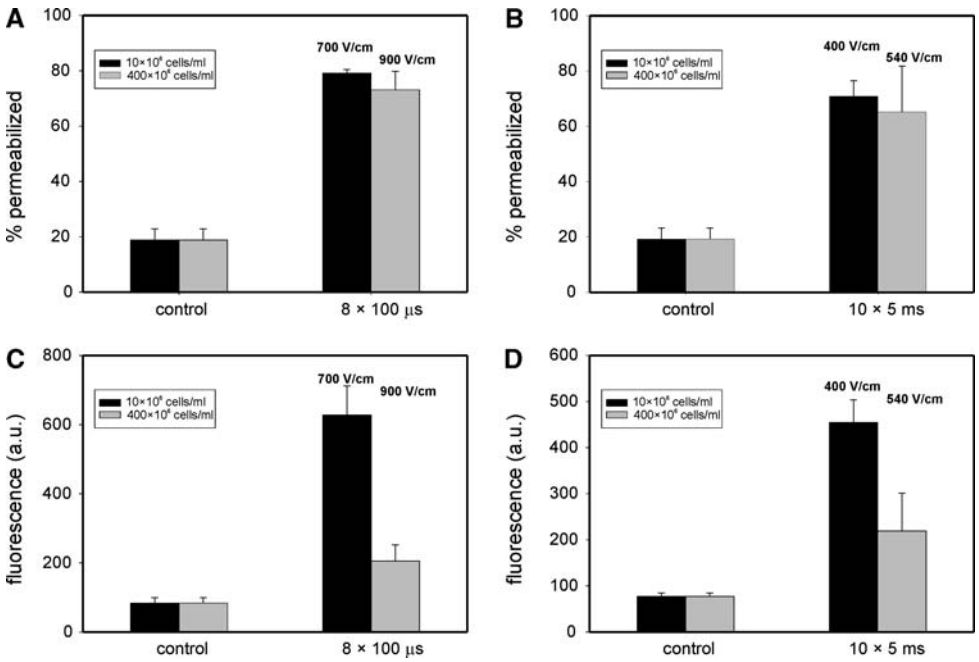

Fig. 6 Permeabilization of the cells in dilute (10×10^6 cells/ml, *black columns*) and dense suspension (400×10^6 cells/ml, *grey columns*) for **a** 8×100 µs, and **b** 10×5 ms pulse protocol, after adjustment of the pulse amplitude to achieve roughly the same fraction of cell permeabilization and after increasing the dye concentration (100 µM in dilute and 156 µM in dense cell suspension) to account for the volume occupied by the cells. Fluorescence of the cells for **c** 8×100 µs and **d** 10×5 ms pulse protocol, for the same pulse parameters and dye concentrations as in **a** and **b**. Each column represents the mean ± SD ($n = 3$)

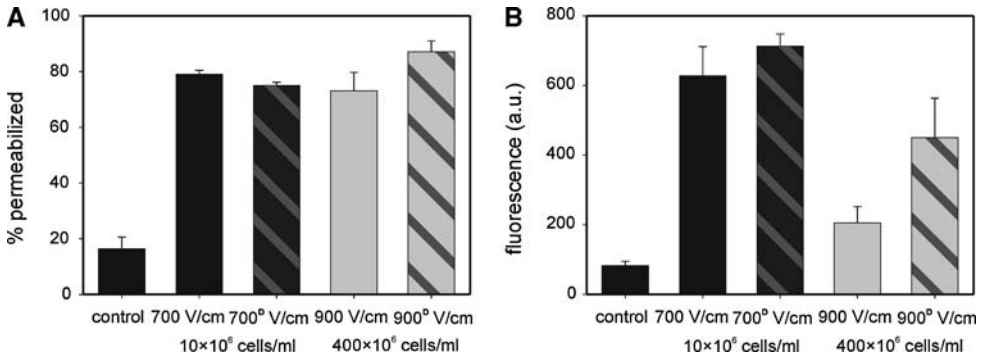

Fig. 7 The influence of the dilution of cell suspension immediately after electropermeabilization. **a** Permeabilization, and **b** fluorescence of the cells in 10×10^6 cells/ml suspension (700 V/cm, *black columns*) and 400×10^6 cells/ml suspension (900 V/cm, *grey columns*) for 8×100 µs pulse protocol. *Hatched columns* represent permeabilization and the fluorescence of the cells that were diluted in 1 ml of pulsing buffer immediately after permeabilization (also denoted with letter D in superscript). Each column represents the mean ± SD ($n = 3$)

Resealing after electropermeabilization

The experiment was performed at 25°C by addition of PI at different times after permeabilization.

First, the resealing of the cells in 10×10^6 cells/ml suspension was determined (black columns in Fig. 8a, b). The fraction of permeabilized cells gradually decreases with time, drops to 50% of the initial value approximately 3 min after permeabilization, and returns to the control value (complete resealing) 7 min after permeabilization (Fig. 8a, b). The fluorescence, on the other hand, decreases sharply in the first 10 s after permeabilization, while the following decrease in the fluorescence is more moderate (Fig. 8c, d). The same trend was observed for both pulse protocols (short or long pulse duration).

Second, the resealing of cells in 400×10^6 cells/ml suspension was determined and compared with resealing in 10×10^6 cells/ml suspension. The resealing was measured at three specific times after permeabilization (0 s, 3, and 7 min), at which approximately 0 50 and 100% of cells in 10×10^6 cells/ml suspension were detected as resealed, respectively. According to the results shown in Fig. 8 , the fraction of permeabilized cells in 400×10^6 cells/ml suspension decreases with time more slowly than in 10×10^6 cells/ml suspension.

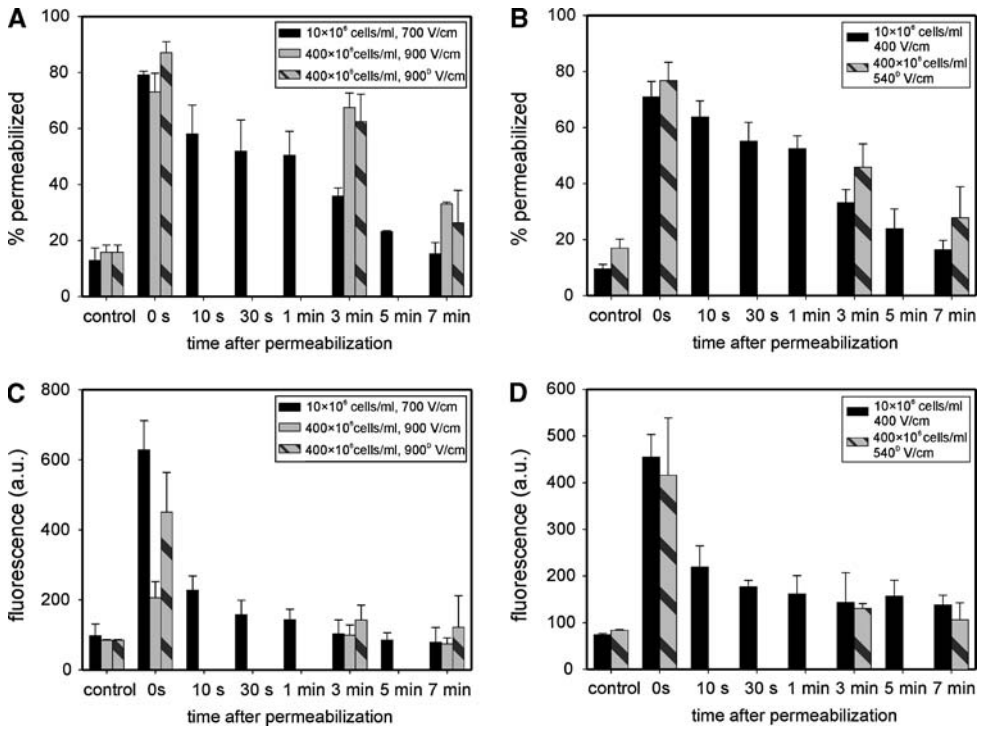

Fig. 8 Resealing after permeabilization. **a** Permeabilization of cells at different times after pulse delivery for 8×100 μs pulse protocol, and **b** for 10×5 ms pulse protocol. *Black columns*, suspension with 10×10^6 cells/ml; *grey columns*, suspension with 400×10^6 cells/ml. **c** Fluorescence of the cells by adding the dye at different times after pulse delivery for 8×100 μs pulse protocol, and **d** for 10×5 ms pulse protocol. The pulse amplitudes and the dye concentrations were the same as in the experiment shown in Fig. 7. Hatched columns represent permeabilization and fluorescence of the cells that were diluted in 1 ml of pulsing buffer immediately after permeabilization (also denoted with letter D in superscript). Each column represents the mean ± SD ($n = 3$)

This effect is more pronounced for short pulses where, for example, the fraction of permeabilized cells in 400×10^6 cells/ml suspension 3 min after permeabilization is approximately 60% in comparison with 35% for cells in 10×10^6 cells/ml suspension. The dilution of the 400×10^6 cells/ml suspension after permeabilization does not considerably influence the detected level of permeabilization (compare the grey and hatched columns in Fig. 8a). The fluorescence of 400×10^6 cells/ml suspension, which was diluted after permeabilization, decreases with time (Fig. 8c, d). Without dilution after permeabilization (grey columns in Fig. 8c), the fluorescence also decreases with time, but from a considerably lower initial value. Three minutes after permeabilization the fluorescence in 10×10^6 and 400×10^6 cells/ml suspension is similar to the fluorescence detected in the control sample.

Discussion

Numerical computations indicated that the transmembrane voltage induced on suspended cells depends on their density in the suspension (Susil et al. 1998; Pavlin et al. 2002). More specifically, as cell density increases, this modifies the peak amplitude of the transmembrane voltage as well as its spatial distribution (Susil et al. 1998; Pavlin et al. 2002). While the deformation of the cosine dependence becomes significant only when the volume fraction of cells exceeds 50% (which is an extreme for suspensions, but a realistic value for cell aggregates or tissues), the decrease in the peak value of the induced transmembrane voltage becomes detectable at volume fractions as low as 10% (Pavlin et al. 2002). Because in our experiments, the volume fractions of cells in suspensions with 10×10^6, 200×10^6, and 400×10^6 cells/ml were approximately 1, 18, and 36%, respectively, we predicted that it was mostly the peak value of the induced transmembrane voltage that was affected by the differences in cell density.

Assuming as usually that the induced transmembrane voltage determines the regions of the cell membrane where electropermeabilization occurs, the increased cell density should, due to lower peak value of the transmembrane voltage, reduce the area of the

permeabilized regions. For cells in suspension, for which the radii are roughly normally distributed [the mean radii being about 6 μm for CHO cells (Golzio et al. 1998)], it would mean that if cell density is increased considerably, some cells may not be permeabilized at all, and those that do will be permeabilized to a smaller geometric extent. The prediction is that the permeabilization of the whole cell suspension assayed both by the percentage of permeabilized cells in the pulsed population and by the extent of electroloading will decrease. Our experimental results of permeabilization as a function of cell density indeed show that the fraction of cell permeabilization and the fluorescence decrease as the cell density increases (Figs. 4a, b; 5a, b), thereby supporting the numerical assumptions qualitatively. Moreover, higher pulse amplitudes were needed to achieve the same fraction of cell permeabilization in dense than in dilute cell suspensions. However, if reduced transmembrane voltage at high cell densities would be the only factor influencing permeabilization, the pulse amplitude achieving the same fraction of permeabilized cells with 400×10^6 cells/ml would have to be by a factor of ~1.13 higher than with 10×10^6 cells/ml (see Fig. 2b). In fact, the ratio between the amplitudes yielding the same permeabilized fractions in our experiments was ~1.29 for 8×100 μs pulses (900 and 700 V/cm), and ~1.35 for 10×5 ms pulses (540 and 400 V/cm). One of the possible reasons for the discrepancy between the numerical and experimental results could be the arrangement of cells in the numerical model of cell suspension (Fig. 2a). Besides the face-centered cubic lattice, other arrangements, such as body cubic or body-centered cubic can be used to model the cell suspension (Pavlin et al. 2002). Computations with these arrangements yield considerably higher decrease in the transmembrane voltages than shown in Fig. 2b. Also, the influence of external cell matrix on the distortion of the electric field around the cells was not taken into account in the calculations. The reduced transmembrane voltage appears not to be the only factor contributing to the reduced permeabilization in dense suspensions, the other factors remain to be elucidated.

The fluorescence results were also affected more than would be expected on the basis of the decreased fraction of permeabilized cells. The fluorescence was thus lower in the dense cell suspension than in the dilute one, even if the pulse amplitudes were chosen to yield roughly the same fraction of permeabilized cells in the two suspensions, and the dye dilution effect was compensated by a higher dye concentration in dense suspension (156 μM) (Fig. 6a–d). We showed with additional experiments that the detected decrease in the fluorescence of dense suspensions was most probably due to cell swelling associated to electropermeabilization (Fig. 7). It has been shown by many authors, including our group on the same CHO strain as used in this paper, that after permeabilization cell size increased (Abidor et al. 1993, 1994; Golzio et al. 1998; Kinosita and Tsong 1977). This occured even if the pulsing medium was isotonic, and it played a significant role in the dye diffusion into the cells. If the suspension was sufficiently dense, an increase in cell size could bring the cells in such suspension into close contact, thereby reducing the free access of dye from extracellular space to the cell membrane and hindering the dye diffusion into the cells (see Eq. 8, Fig. 9). A direct video assay under the microscope showed that the volume of CHO cells (the same WTT clone) can increase by more than 100% during a 10 s permeabilizing pulse train, and cells remain swollen for a few minutes after the pulse (Golzio et al. 1998). This makes it reasonable to believe that our initial volume fraction of cells (36%) could have increased to a limiting value (~75%, Pavlin et al. 2002), where cells are in close contact with each other. The external volume in this case would reduce to 25%. Cell swelling was probably also the main reason for the decrease in electrical conductivity after permeabilization, observed in cell pellets and dense cell suspensions (Abidor et al. 1994; Pavlin et al. 2005).

Recently Canatella et al. (2004) used multicellular spheroids as a simple model of tissue, showing that the uptake of molecules into the cells in the spheroid was lower than the uptake into the same cells when suspended (Canatella et al.). Canatella attributed this to slow diffusion of the dye into the cells in the interior of the spheroid, limited extracellular reservoir and heterogeneous electric field strength. However, our study on dense cell suspensions presented in this paper shows that even if all these effects are accounted for, the dye uptake is still lower in dense suspensions than in dilute ones, and that cell swelling is also a contributing factor. Cell swelling after electropermeabilization could perhaps also occur in tissues and contribute to the reduced uptake.

Our experiments show that the resealing of cells after permeabilization also depends on the density of the suspension. Namely, the cells in dense suspensions resealed more slowly than cells in dilute suspensions (Fig. 8). A possible explanation for slower resealing of cells in dense suspensions is the stress experienced during the addition of the dye (see Materials and methods), because repeated pipetting was needed to homogenize the dye distribution in dense cell suspension. Nevertheless, our protocol was not observed to

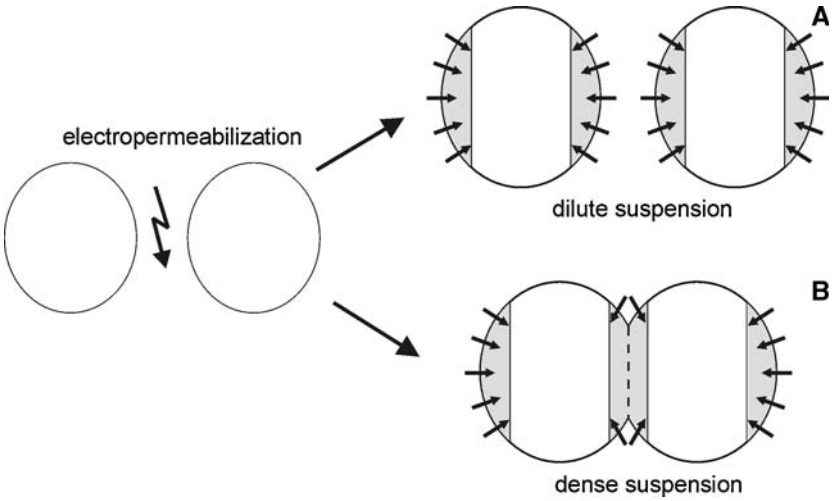

Fig. 9 Cell swelling after permeabilization in **a** dilute suspensions, **b** dense suspensions. Cells after permeabilization increase in their size (cell swelling) due to the fast inflow of water and ions. In contrast, inflow of exogenous molecules, like PI is rather slow. If suspension is sufficiently dense, cells could come into close contact, thereby reducing the free access of dye in extracellular space to the cell membrane and hindering the dye diffusion into the cells (*arrows*). Permeabilized regions of the membranes are marked in grey

damage the cells, as no lysis was detected in the long term. Li et al. (1999) suggested that at high cell densities, the restriction of nutrients supply should slow cell recovery and induce a decrease in viability. Such an interpretation did not seem to apply in our case, as resealing was fast and we observed that the exchange across the membrane was decreased. This implies that ATP cytoplasmic level was not affected significantly (and should not affect the resealing process as reported for starved cells) (Rols et al. 1998). Osmotic effects appeared more relevant. It was observed that under hyperosmolar conditions the membrane resealing after electropermeabilization is slower than under isoosmolar conditions (Rols et al. 1990). In the present experiments, swelling was a fast process, meaning that the water inflow was rapid. In contrast, inflow of exogenous molecules (sucrose, PI) was shown to be rather slow (minutes after permeabilization) (Sixou and Teissié 1993). As a conclusion, permeabilization by inducing cell swelling changed the osmotic pressure of the extracellular buffer. This means that cells in dense suspensions were pulsed in a buffer with an increasing osmolarity during the pulse train. Hyperosmolarity was therefore present and should support the observation of a slower resealing. Such an explanation is further supported by our previous observations of a lower extent of permeabilization and of electroloading (mean fluorescence) in hyperosmolar pulsing buffers (Rols et al. 1990).

Experiments in this study were performed with propidium iodide, a small molecule that enters the cell largely by diffusion. For molecules of similar size the results are predicted to be similar (Sixou and Teissié 1993). For larger molecules, such as DNA, which enter the cells by a different process than diffusion, the uptake would probably be affected at the level of the diffusion in the bulk (Golzio et al. 2002).

In summary, our results show that cell permeabilization in dense suspensions differs considerably from that in dilute suspensions. The differences mostly arise as a consequence of mutual electrical shielding of cells, which causes a decrease in the amplitude of transmembrane voltage on such cells. These observations provide the experimental support for previous theoretical studies. The findings obtained on dense suspensions could contribute to a better understanding of the mechanisms of tissue electropermeabilization, where mutual shielding of cells (cells in tissues are in close contact) is one of the important factors influencing the permeabilization of cells. In this aspect, dense cell suspensions with an intact extracellular matrix (such as the CHO cells used in this study) are in their properties closer to tissues than dilute suspensions, and as such present a suitable model for tissues exhibiting isotropic characteristics. However, tissues showing anisotropic characteristics (e.g. muscles), or tissues which are a complex assembly of cells considerably different in shape from those in suspensions, cannot be modeled with dense suspensions of spherical cells. The second conclusion is that cell swelling is cross-reacting with electropermeabilization and this phenomenon should be present also in tissues.

Acknowledgments The author (G. P.) would like to thank Dr. M. Golzio, Dr. M. P. Rols and Dr. B. Gabriel for their valuable discussions during the experiments, and Ms. C. Millot for her help with cell cultures. This work was supported by the Ministry of the Higher Education and Science of the Republic of Slovenia. G. P. was also a recipient of a scholarship from the French government. The two institutes are partners in a Slovenian-French CNRS PICS program.

References

Abidor IG, Barbul AI, Zhelev DV, Doinov P, Bandrina IN, Osipova EM, Sukharev SI (1993) Electrical properties of cell pellets and cell electrofusion in a centrifuge. Biochim Biophys Acta 1152:207–218

Abidor IG, Li LH, Hui SW (1994) Studies of cell pellets: II. Osmotic properties, electroporation, and related phenomena: membrane interactions. Biophys J 67:427–435

Barnett A, Weaver JC (1991) Electroporation: a unified, quantitative theory of reversible electrical breakdown and rupture. Bioelectrochem Bioenerg 25:163–182

Canatella PJ, Black MM, Bonnichsen DM, McKenna C, Prausnitz MR (2004) Tissue electroporation: quantification and analysis of heterogeneous transport in multicellular environments. Biophys J 86:3260–3268

Čemažar M, Grošel A, Glavač D, Kotnik V, Škobrne M, Kranjc S, Mir LM, Andre F, Opolon P, Serša G (2003) Effects of electrogenetherapy with p53wt combined with cisplatin on survival of human tumor cell lines with different p53 status. DNA Cell Biol 22:765–775

Fattori E, Cappelletti M, Zampaglione I, Mennuni C, Calvaruso F, Arcuri M, Rizzuto G, Costa P, Perretta G, Ciliberto G, La Monica N (2005) Gene electro-transfer of an improved erythropoietin plasmid in mice and non-human primates. J Gene Med 7:228–236

Golzio M, Mora MP, Raynaud C, Delteil C, Teissié J, Rols MP (1998) Control by osmotic pressure of voltage-induced permeabilization and gene transfer in mammalian cells. Biophys J 74:3015–3022

Golzio M, Teissié J, Rols MP (2002) Direct visualization at the single-cell level of electrically mediated gene delivery. Proc Natl Acad Sci 99:1292–1297

Gothelf A, Mir LM, Gehl J (2003) Electrochemotherapy: results of cancer treatment using enhanced delivery of bleomycin by electroporation. Cancer Treat Rev 29:371–387

Grosse C, Schwan HP (1992) Cellular membrane potentials induced by alternating fields. Biophys J 63:1632–1642

Kinosita K, Tsong TY (1977) Formation and resealing of pores of controlled sizes in human erythrocyte membrane. Nature 268:438–441

Kotnik T, Bobanović F, Miklavčič D (1997) Sensitivity of transmembrane voltage induced by applied electric fields—a theoretical analysis. Bioelectrochem Bioenerg 43:285–291

Li LH, Ross P, Hui SW (1999) Improving electrotransfection efficiency by post pulse centrifugation. Gene Ther 6:364–372

Mir LM, Orlowski S (1999) Mechanisms of electrochemotherapy. Adv Drug Deliver Rev 35:107–118

Neumann E, Ridder MS, Wang Y, Hofschneider PH (1982) Gene transfer into mouse lyoma cells by electroporation in high electric fields. EMBO J 1:841–845

Neumann E, Toensing K, Kakorin S, Budde P, Frey J (1998) Mechanism of electroporative dye uptake by mouse B cells. Biophys J 74:98–108

Neumann E, Kakorin S, Toensing K (1999) Fundamentals of electroporative delivery of drugs and genes. Bioelectrochem Bioenerg 48:3–16

Okino M, Mohri H (1987) Effects of high-voltage electrical impulse and an anticancer drug on in vivo growing tumors. Jpn J Cancer Res 78:1319–1321

Pauly H, Schwan HP (1959) Über die impedanz einer suspension von kugelförmigen teilchen mit einer schale. Z Naturforsch 14B:125–131

Pavlin M, Pavšelj N, Miklavčič D (2002) Dependence of induced transmembrane potential on cell density, arrangement, and cell position inside a cell system. IEEE Trans Biomed Eng 49:605–612

Pavlin M, Kandušer M, Reberšek M, Pucihar G, Hart FX, Magjarević R, Miklavčič D (2005) Effect of cell electroporation on the conductivity of a cell suspension. Biophys J 88:4378–4390

Pucihar G, Kotnik T, Valič B, Miklavčič D (2006) Numerical determination of transmembrane voltage induced on irregularly shaped cells. Annals Biomed Eng 34:642–652

Rols MP, Teissié J (1990) Electropermeabilization of mammalian cells: quantitative analysis of the phenomenon. Biophys J 58:1089–1098

Rols MP, Teissié J (1998) Electropermeabilization of mammalian cells to macromolecules: control by pulse duration. Biophys J 75:1415–1423

Rols MP, Dahhou F, Mishra KP, Teissie J (1990) Control of electric field induced cell membrane permeabilization by membrane order. Biochemistry 29:2960–2966

Rols MP, Delteil C, Golzio M, Teissié J (1998) Control by ATP and ADP of voltage-induced mammalian-cell-membrane permeabilization, gene transfer and resulting expression. Eur J Biochem 254:382–388

Šatkauskas S, Bureau MF, Puc M, Mahfoudi A, Scherman D, Miklavčič D, Mir LM (2002) Mechanisms of in vivo DNA electrotransfer: respective contributions of cell electropermeabilization and DNA electrophoresis. Mol Ther 5:133–140

Šatkauskas S, Batiuškaite D, Šalomskaite-Davalgiene S, Venslauskas MS (2005) Effectiveness of tumor electrochemotherapy as a function of electric pulse strength and duration. Bioelectrochemistry 65:105–111

Schmeer M, Seipp T, Pliquett U, Kakorin S, Neumann E (2004) Mechanism for the conductivity changes caused by membrane electroporation of CHO cell-pellets. PCCP 6:5564–5574

Schwan HP (1957) Electrical properties of tissue and cell suspensions. Adv Biol Med Phys 5:147–209

Serša G, Čemažar M, Miklavčič D (1995) Antitumor effectiveness of electrochemotherapy with cis-diammindichloroplatinum(II) in mice. Cancer Res 55:3450–3455

Sixou S, Teissié J (1993) Exogeneous uptake and release of molecules by electroloaded cells: a digitized videomicroscopy study. Bioelectrochem Bioenerg 31:237–257

Susil R, Šemrov D, Miklavčič D (1998). Electric field induced transmembrane potential depends on cell density and organization. Electro Magnetobiol 17:391–399

Teissié J, Eynard N, Gabriel B, Rols MP (1999) Electropermeabilization of cell membranes. Adv Drug Deliver Rev 35:3–19

Tsong TY (1991) Electroporation of cell membranes. Biophys J 60:297–306

Weaver JC, Chizmadzhev YA (1996) Theory of electroporation: a review. Bioelectrochem Bioenerg 41:135–160